Thermodynamics

DOI: 10.1002/anie.201405648

Aligning Electronic and Protonic Energy Levels of Proton-Coupled Electron Transfer in Water Oxidation on Aqueous TiO_2**

Jun Cheng, Xiandong Liu, John A. Kattirtzi, Joost VandeVondele, and Michiel Sprik*

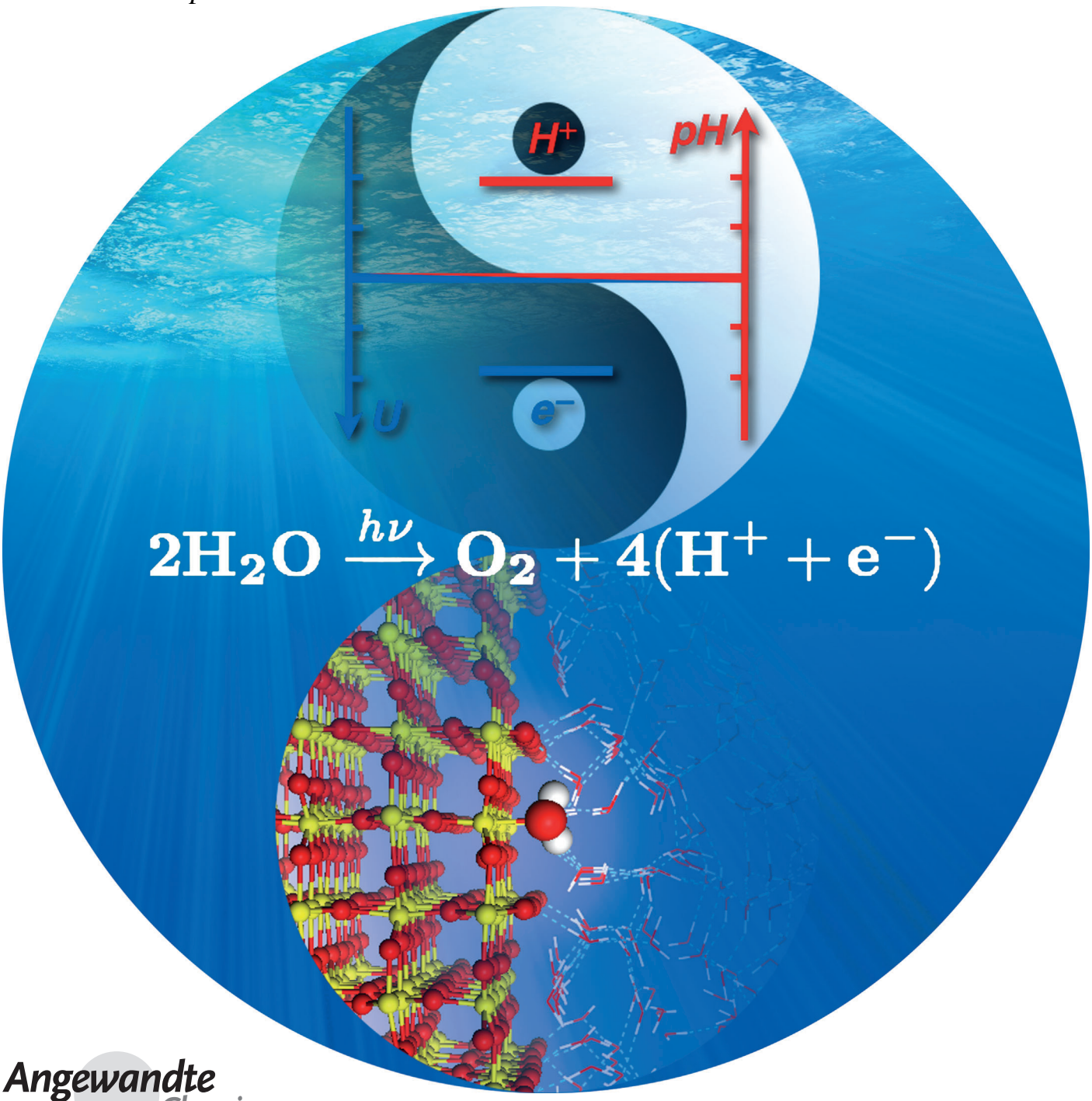

Abstract: *The high overpotential in water oxidation on anodes is a limiting factor for the large-scale application of photoelectrochemical cells. To overcome this limitation, it is essential to understand the four proton-coupled electron transfer (PCET) steps in the reaction mechanism and their implications to the overpotential. Herein, a simple scheme to compute the energies of the PCET steps in water oxidation on the aqueous TiO_2 surface using a hybrid density functional is described. An energy level diagram for fully decoupled electron- and proton-transfer reactions in which both electronic and protonic levels are placed on the same potential scale is also described. The level diagram helps to visualize the electronic and protonic components of the overpotential, and points out what are needed to improve. For TiO_2, it is found that its catalytic activity is due to aligning the protonic energy levels in the PCET steps, while improving the activity requires also aligning the electronic levels.*

Photoelectrochemical splitting of water is a direct and attractive approach for utilization of sunlight by converting solar energy into chemical fuel, namely hydrogen. The reverse reaction occurs in fuel cells where the stored chemical energy is released in the form of electricity with water as the byproduct. This step completes the pollution-free cycle which lies at the core of the blueprint of a hydrogen economy. To achieve this system, one of the major technological issues which has to be overcome is the lack of efficient electrode materials which are low cost and have a long lifetime. The inefficiencies are often attributed to the high overpotentials associated with water oxidation at anodes in solar cells and oxygen reduction at cathodes in fuel cells, thus leading to high energy loss in this cycle. Therefore, there is a clear need to gain a fundamental understanding of the overpotentials which may guide the search for more efficient electrode materials.

The thermodynamic overpotential model popularized by Nørskov, Rossmeisl, and co-workers[1] has made a considerable contribution to such an understanding. It also provides a simple yet powerful theoretical method for estimating reaction overpotentials using density functional theory (DFT) calculations, and thus has been widely used in studying metallic electrocatalysts (e.g. Pt and RuO_2)[2,3] and semiconducting photocatalysts (e.g. TiO_2 and Fe_2O_3).[4–6] In this model, taking water oxidation as an example $[2\,H_2O(l) \rightarrow O_2(g) + 4\,(H^+ + e^-)]$, it is assumed that the reaction proceeds as four successive steps of concerted electron and proton transfers (i.e. dehydrogenation). The dehydrogenation energies are computed using DFT with reference to a gas-phase H_2 molecule. They are equivalent to redox potentials of the dehydrogenation reactions versus the standard hydrogen electrode (SHE). For an ideal catalyst, the dehydrogenation potentials for each of the four steps should be the same. Note that they are equal to 1.23 V (the standard redox potential of overall water oxidation reaction) only if the non-electrochemical steps involved (i.e. adsorption/desorption and O–O bond formation) have negligible energy contributions.[7,8] Any deviation from the ideal will lead to a thermodynamic overpotential.

In water oxidation, electron and proton transfer can occur not only in a concerted manner but also in sequence. These two alternative mechanisms form the reaction pathways of proton-coupled electron transfer (PCET), as illustrated in a triangular scheme in Figure 1. It is a well-known concept in physical organic chemistry, and has been extensively studied for homogeneous and biological systems.[9–12] In contrast, heterogeneous PCET reactions are less well documented.[13,14] In a recent review,[15] Koper indicated that a *concerted* mechanism may be favored on strongly interacting catalysts like platinum, while a *decoupled* mechanism is more likely on weakly interacting surfaces like gold. The latter should be also expected for semiconducting oxides. In decoupled electron- and proton-transfer reactions such as water oxidation on oxide catalysts, it is very important to know the precise thermochemistry of the PCET steps to understand the overpotentials. Herein, we report the reaction energies of the PCET steps of water oxidation on an important heterogeneous interface. The system we study is the aqueous rutile

[*] Dr. J. Cheng
Department of Chemistry, University of Aberdeen
Aberdeen AB24 3UE (UK)
E-mail: jcheng@abdn.ac.uk
Dr. X. Liu
State Key Laboratory for Mineral Deposits Research
School of Earth Science and Engineering, Nanjing University
Nanjing 210093 (P.R. China)
Dr. X. Liu, Dr. J. A. Kattirtzi, Prof.Dr. M. Sprik
Department of Chemistry, University of Cambridge
Cambridge CB2 1EW (UK)
Dr. J. VandeVondele
Department of Materials, ETH Zurich
Wolfgang-Pauli-Strasse 27, CH-8093 Zurich (Switzerland)

[**] The calculations in this work have been performed on HECToR and ARCHER, the UK's high-end computing resource funded by the Research Councils, as part of a grant to the UKCP consortium, as well as on High Performance Computing Cluster Maxwell at University of Aberdeen.

Supporting information for this article is available on the WWW under http://dx.doi.org/10.1002/anie.201405648.

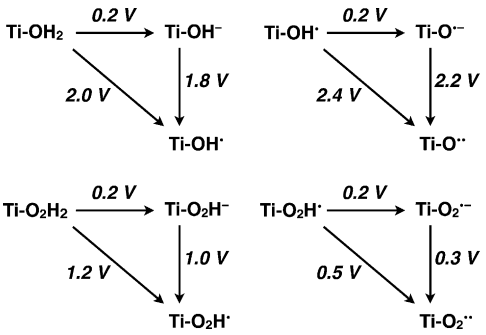

Figure 1. The energetics of the four PCET steps in water oxidation on rutile TiO_2(110) as computed using the hybrid HSE06. The acidities (horizontal) are converted into a potential scale in volts (1 pK_a unit is equivalent to 59 mV at room temperature), and the oxidation (vertical) and dehydrogenation (diagonal) reaction energies are expressed as potentials versus the SHE. The symbols denote the reaction intermediates on the five-coordinated terminal titanium site. The computed energies and their conversion into the PCET potentials are summarized in Table S1 in the Supporting Information.

TiO_2(110) surface, and the reaction energies have been computed using a new method which we have developed. Furthermore, we utilize an appealing concept, of an acid-base scale developed in solid-state chemistry,[16–18] to elucidate the significance of the thermochemistry of PCET to thermodynamic overpotentials by aligning the electronic and protonic energy levels on the same potential-energy scale.

The oxidation of water adsorbed on the five-coordinated terminal titanium site in a periodic 4×2 five tri-layer-slab model (80 TiO_2 units) has been computed using the hybrid functional HSE06.[19] The program we use is CP2K,[20] and the calculations using the hybrid functional have been performed by using an auxiliary density matrix method recently developed and implemented in CP2K.[21] The same computational setup has been used in the previous studies[13,22] and the detailed descriptions can be found in the Supporting Information. The computed reaction energies are illustrated in the four PCET triangles in Figure 1. All the energies are presented on a potential scale. We refer to them as deprotonation potentials (i.e. 59 mV = 1 pK_a unit) for acid-base reactions (horizontal), oxidation potentials for redox reactions (vertical), and dehydrogenation potentials for dehydrogenation reactions (diagonal). The latter two are referenced to the SHE.

One of the major difficulties in computing the heterogeneous PCET energies is to obtain physically meaningful energies for charged species under periodic boundary conditions.[23] The approach we developed previously referenced the computed energies to a computational SHE, by comparing to the solvation free energy of a proton (i.e. the proton affinity of an aqueous water molecule). The free energies for reversible insertion of an electron/proton are calculated by combining ab inito molecular dynamics and free-energy perturbation theory.[23,24] The accuracy of our method has been extensively tested for both homogeneous solutions[23] and solid-liquid interfaces[13,25,26] in the previous work. The error of the acidities is 1–2 pK_a units, and for redox potentials it is on the order of 0.1–0.2 V using the hybrid functional HSE06. In this work, we develop a new scheme in which an internal reference, namely, the proton affinity of a surface bridge O site instead of that of an aqueous water molecule, is used. The detailed description and the validation of this scheme, as well as a brief outline of our method for computing pK_a values and redox potentials, are given in the Supporting Information. The values reported in Figure 1 have been computed with this scheme. The space charge layer and electric double layer (EDL) are not included in our simulation model, and thus the state of our model corresponds to the flat band potential at the pH equal to the point of zero charge (PZC) of the oxide. The effects of double layers can be taken into account by adding analytical activity terms. In particular, the pH conditions deviating from PZC can lead to the buildup of EDL and shifts in the PCET potentials.[13,27] This EDL effect is discussed in some detail in Section S6 in the Supporting Information.

To obtain accurate energies in Figure 1, it is important to ensure the calculated intermediates have the correct spin states. In the early computational studies of water oxidation on semiconductors, the radical nature of the reaction intermediates was not always taken into account. This is usually not an issue for metallic electrocatalysts owing to the quenching of the spin by the partially filled electronic bands. However, for semiconducting photocatalysts, the spin quenching is often incomplete and the intermediates, by and large, remain radicals. The degree of spin quenching is strongly dependent on the positions of the band edges of the semiconductors studied. Density functionals at the level of generalized gradient approximation (GGA) suffer from large errors (up to a few eV) in computing the band positions because of the delocalization error.[28] The serious consequence is that GGA functionals make semiconductors more metal-like, thus leading to over-quenched spin states and inaccurate reaction energies. This technical but important issue has been investigated and discussed in detail in our recent work.[13,29] Fortunately, the hybrid functional HSE06 gives an accurate band alignment for TiO_2, and therefore should describe these radical states reliably.[13] Their structures are shown in Figure 2, and the visualization of spin densities confirms that the correct spin states have been obtained. In particular, the Mulliken spin population shows that the adsorbed O (spin 1.84) and O_2 (spin 1.98) indeed have triplet ground states, as expected.

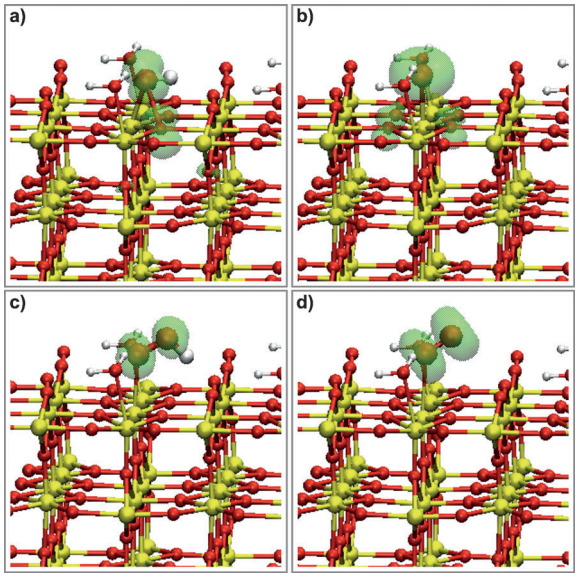

Figure 2. The structures of key intermediates in water oxidation on rutile TiO_2(110): a) $OH^{\bullet}$; b) $O^{\bullet\bullet}$; c) $HO_2^{\bullet}$; d) $O_2^{\bullet\bullet}$. Ti yellow, O red, and H white. The active species are highlighted with larger atom sizes. The spin densities of the surface radicals are visualized by green isosurfaces with a density threshold of 3×10^{-3}.

It is not possible to carry out a full comparison of the PCET energies between computation and experiment as they are generally very difficult to measure. To the best of our knowledge, our computed energies in Figure 1, that is, the oxidation potential of surface $OH^-/OH^{\bullet}$ and the deprotonation potential of surface $OH^{\bullet}$, are in good agreement with the limited experimental values available from kinetic measurements.[30,31] According to Figure 1, it is evident that all the deprotonation steps (horizontal reactions) have moderate

reaction energies, thus indicating medium pK_a values for all four surface intermediates (i.e. adsorbed H_2O, $OH^{\bullet}$, H_2O_2, and $HO_2^{\bullet}$). This data confirms that the PCET steps most likely proceed in a decoupled electron- and proton-transfer route, as a concerted mechanism usually takes place to avoid unstable intermediates in the decoupled pathways, which appears not the case for water oxidation on TiO_2 from our calculations. Also, the second PCET step ($OH^{\bullet} \rightarrow O^{\bullet\bullet}$) has the highest reaction energy. In particular, the oxidation step ($O^{\bullet-} \rightarrow O^{\bullet\bullet}$) has an extreme redox potential of 2.2 V. This value indicates that the O atom adsorbed on the terminal titanium site should not be involved in the reaction mechanism on TiO_2 as the $OH^{\bullet}$ radicals produced in the first PCET step can couple with each other to form H_2O_2. By omitting the second PCET step, the first dehydrogenation step can be regarded as being potentially limiting.

To further demonstrate the importance of the PCET energies in understanding the thermodynamic overpotential, we introduce the concept of an acid-base scale developed by Maier to illustrate the thermodynamics of point defects in ionic solids.[16–18] He noticed the isomorphism in the thermodynamic treatment between ionic and electronic charge carriers, and proposed representation of the thermodynamics of ionic defects using energy level diagrams similar to the electronic energy level diagrams used in semiconductor physics. In acid-base chemistry, H^+(aq) is analogous to the ionic charge carrier in the defect chemistry of ionic solids, and thus the pK_a values can be shown as protonic energy levels in a similar manner. Furthermore, he suggested that the electronic and ionic components can be linked by presenting both energy levels in the same energy scale.[18] For interested readers, we refer you to Maier's original papers[16–18] for more detail.

Inspired by this concept, we simultaneously align the electronic and protonic energy levels of the four PCET steps for water oxidation on TiO_2 (solid lines) and in aqueous solution (dashed lines), as shown in Figure 3. In this plot, the redox potential axis (red) points down as usual, while the acidity axis (blue) points up. The zeros of both axes are, however, aligned and this is essential because it ensures the gaps between electronic (in red) and protonic (in blue) levels, denoted by black arrows in Figure 3, are equal to dehydrogenation potentials. This equality is required by Hess's Law, which guarantees that dehydrogenation potentials are equal to the sum of deprotonation and oxidation potentials in the PCET triangles. Note that the redox potentials can span a potential range of more than 2 V, which is much larger than the acidity scale. The relatively smaller span of the acidity scale is due to the fact that the usual active pK_a window (0–14) in aqueous solution only amounts to a potential range of about 0.8 V.

Separation of dehydrogenation into deprotonation and oxidation allows examination of the protonic and electronic components of the thermodynamic overpotentials. This separation is the key advantage of knowing the thermochemistry of the PCET steps. From this perspective, the requirement for an ideal catalyst is stricter. Not only the dehydrogenation potentials for all steps are equal, but also that of each of the two components, the deprotonation and oxidation potentials, should be the same. These equalities can be derived by following a thermodynamic argument similar to that of Nørskov, Rossmeisl and co-workers.[1] As also indicated by Koper,[15] for an optimal catalyst all steps in the mechanism, both electrochemical (i.e. oxidation) and non-electrochemical (e.g. deprotonation), must be thermodynamically neutral or downhill. The thermodynamic driving forces for oxidation and deprotonation are the electronic and protonic electrochemical potentials, respectively, which are independent of each other and provided externally by varying voltage on the electrode and pH in the solution. Note that in photocatalysis the voltage should be referred to as the quasi-fermi level[32] of excited holes under illumination. This thermodynamic requirement for decoupled electron- and proton-transfer reactions can be better illustrated by the level diagram in Figure 3: for the four PCET steps in water oxidation, the blue protonic levels should be aligned, as should the red electronic levels. The maximum deviations from the respective average levels give the estimates of the protonic and electronic components of the thermodynamic overpotentials. It is worth pointing out that in electrochemistry the term overpotential refers to the electrochemical potential of electrons, and here we extend it to also the protonic potential.

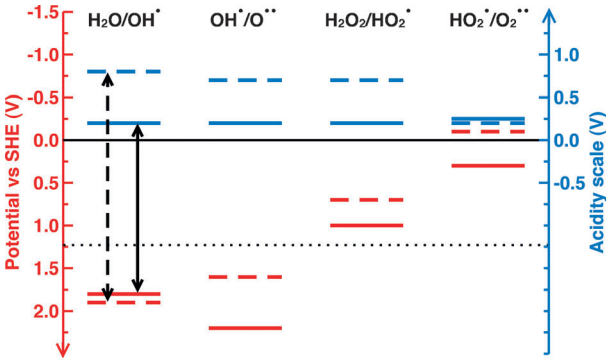

Figure 3. Electronic and protonic energy level diagram for the four PCET steps in water oxidation. Red and blue represent electronic and protonic levels, respectively. Solid lines are the levels calculated on TiO_2. The respective experimental levels in aqueous solution, denoted by dashed lines, are also included for comparison (numerical values are shown in Figure S5 in the Supporting Information). The black arrows stand for the dehydrogenation potentials. The dotted black line indicates the standard redox potential (1.23 V) of the overall water oxidation reaction.

With the help of this level diagram, we can clearly show the origin of the catalytic activity/inactivity of TiO_2 by comparing the energy levels on TiO_2 (solid lines) with those of a water solution (dashed lines)(Figure 3). We therefore draw the following conclusions:

1. The adsorption on TiO_2 greatly reduces the first dehydrogenation potential (potential limiting step) by 0.7 V, and is mainly attributed to the increased acidity of water on TiO_2.[13] This catalytic effect can be readily visualized in the level diagram. The solid black arrow denoting the dehydrogenation potential on TiO_2 is shorter than the dashed one for that in water, and this shortening, to a large extent, results from the lowering of the blue protonic level, and less so from the lifting of the red electronic level.

2. More importantly, the protonic levels are almost perfectly aligned by TiO_2, which is in contrast to the levels in solution as they spread over a range of about 0.6 V. This alignment indicates that at an appropriate pH condition there will be no or minimal thermodynamical overpotential component coming from the deprotonation.
3. The inefficiency of TiO_2 results from the scattered electronic levels. Even if the second PCET step is omitted, the electronic levels still range from 0.3 to 1.7 V. Nonetheless, this range is better than in water where the span of electronic levels is about 2 V.

To summarize, we report the reaction energies of the four PCET steps of water oxidation on an aqueous rutile TiO_2 surface. These energies have been computed using a hybrid functional, and the accuracy has been carefully benchmarked. Furthermore, we introduce the concept of electronic and protonic energy levels to study PCET reactions, and propose a level diagram to visualize their thermodynamics. Within this new level scheme, it is straightforward to see the electronic and protonic components of the thermodynamic overpotentials, and understand the activity/inactivity of catalytic materials. It is expected that this level diagram can be insightful not only for heterogeneous interfaces but also for homogeneous systems. As for water oxidation on TiO_2, we find that TiO_2 is able to align the protonic levels as desired, while it fails to align the electronic ones. The open challenge is thus the alignment of the electronic levels.

Received: May 26, 2014
Published online: July 23, 2014

Keywords: computational chemistry · heterogeneous catalysis · photochemistry · proton transfer · thermodynamics

[1] J. K. Nørskov, J. Rossmeisl, A. Logadottir, L. Lindqvist, J. R. Kitchin, T. Bligaard, H. Jónsson, *J. Phys. Chem. B* **2004**, *108*, 17886 – 17892.
[2] J. Rossmeisl, Z.-W. Qu, H. Zhu, G.-J. Kroes, J. K. Nørskov, *J. Electroanal. Chem.* **2007**, *607*, 83 – 89.
[3] Y.-H. Fang, Z.-P. Liu, *J. Am. Chem. Soc.* **2010**, *132*, 18214 – 18222.
[4] A. Valdés, Z. W. Qu, G. J. Kroes, J. Rossmeisl, J. K. Nørskov, *J. Phys. Chem. C* **2008**, *112*, 9872 – 9879.
[5] Y.-F. Li, Z.-P. Liu, L. Liu, W. Gao, *J. Am. Chem. Soc.* **2010**, *132*, 13008 – 13015.
[6] P. Liao, J. a. Keith, E. a. Carter, *J. Am. Chem. Soc.* **2012**, *134*, 13296 – 13309.
[7] F. Tian, A. B. Anderson, *J. Phys. Chem. C* **2011**, *115*, 4076 – 4088.
[8] A. B. Anderson, *Phys. Chem. Chem. Phys.* **2012**, *14*, 1330 – 1338.
[9] J. J. Warren, T. a. Tronic, J. M. Mayer, *Chem. Rev.* **2010**, *110*, 6961 – 7001.
[10] S. Hammes-Schiffer, A. a. Stuchebrukhov, *Chem. Rev.* **2010**, *110*, 6939 – 6960.
[11] J.-M. Savéant, *Energy Environ. Sci.* **2012**, *5*, 7718 – 7731.
[12] M. T. M. Koper, *Phys. Chem. Chem. Phys.* **2013**, *15*, 1399 – 1407.
[13] J. Cheng, M. Sulpizi, J. VandeVondele, M. Sprik, *ChemCatChem* **2012**, *4*, 636 – 640.
[14] J. N. Schrauben, R. Hayoun, C. N. Valdez, M. Brasten, L. Fridley, J. M. Mayer, *Science* **2012**, *336*, 1298 – 1301.
[15] M. T. M. Koper, *Chem. Sci.* **2013**, *4*, 2710.
[16] J. Maier, *Chem. Eur. J.* **2001**, *7*, 4762 – 4770.
[17] J. Z. Maier, *Z. Anorg. Allg. Chem.* **2004**, *630*, 2562 – 2568.
[18] J. Maier, *Ann. Phys.* **2006**, *15*, 469 – 479.
[19] a) J. Heyd, G. E. Scuseria, M. Ernzerhof, *J. Chem. Phys.* **2003**, *118*, 8207 – 8215; b) A. V. Krukau, O. A. Vydrov, A. F. Izmaylov, G. E. Scuseria, *J. Chem. Phys.* **2006**, *125*, 224106.
[20] J. VandeVondele, M. Krack, F. Mohamed, M. Parrinello, T. Chassaing, J. Hutter, *Comput. Phys. Commun.* **2005**, *167*, 103 – 128.
[21] M. Guidon, J. Hutter, J. VandeVondele, *J. Chem. Theory Comput.* **2010**, *6*, 2348 – 2364.
[22] J. Cheng, J. VandeVondele, M. Sprik, *J. Phys. Chem. C* **2014**, *118*, 5437 – 5444.
[23] J. Cheng, M. Sulpizi, M. Sprik, *J. Chem. Phys.* **2009**, *131*, 154504.
[24] J. Cheng, M. Sprik, *Phys. Chem. Chem. Phys.* **2012**, *14*, 11245 – 11267.
[25] J. Cheng, M. Sprik, *J. Chem. Theory Comput.* **2010**, *6*, 880 – 889.
[26] J. Cheng, M. Sprik, *Phys. Rev. B* **2010**, *82*, 81406.
[27] J. Cheng, M. Sprik, *J. Phys. Condens. Matter* **2014**, *26*, 244108.
[28] A. J. Cohen, P. Mori-Sánchez, W. Yang, *Science* **2008**, *321*, 792 – 794.
[29] R. V. Mom, J. Cheng, M. T. M. Koper, M. Sprik, *J. Phys. Chem. C* **2014**, *118*, 4095 – 4102.
[30] D. Lawless, N. Serpone, D. Meisel, *J. Phys. Chem.* **1991**, *95*, 5166 – 5170.
[31] S. Tojo, T. Tachikawa, M. Fujitsuka, T. Majima, *Chem. Phys. Lett.* **2004**, *384*, 312 – 316.
[32] H. Gerischer, *J. Electroanal. Chem.* **1977**, *82*, 133 – 143.

